EXPERIMENTAL INVESTIGATION OF THREE DIMENSIONAL SEPARATED FLOW OVER A BODY OF REVOLUTION AT HIGH ANGLES OF ATTACK

Tadateru Ishide [1)], Nobuhide Nishikawa [2)] and Fumihiko Mikami [2)]
1)Kisarazu National College of Technology , 2-11-1,kiyomidai-higashi , Kisarazu City
2)Chiba University , 1-33 , yayoi-cho , inage-ku , Chiba City

Key Words : *Separated Flow , Laser Light Sheet Method , Smoke Visualization Technique*

Abstract

The flow in the cross-flow separation of an axisymmetric paraboloid at 30, 40 and 50 deg angle of attack has been investigated experimentally by smoke visualization technique and hot wire anemometer. Reynolds numbers are 9.0×10^3 and 1.8×10^4 referred to the base diameter. Laser light sheet method is used in studying the structure of the vortices in cross-sectional flow. The development of streamwise vortices in each section of the body is visualized. X-type probe was used to measure three dimensional velocity fields over the axisymmetric paraboloid. Velocity fluctuations at sampling time of 4kHz have been also evaluated. The extent of longitudinal vortices, such as main-, primary- and secondary vortices, and the change of r.m.s. value in various cross-sections are presented. The variation of vortex patterns is shown for each cross-section, angle of attack and Reynolds number. It has been confirmed that each streamwise vortex is related to the velocity fluctuations.

1 Introduction

Flow separation from a body surface plays a dominant role in the aerodynamic performance of many systems. Because it nearly always has detrimental effects, separation has been - and still is - the subject of many studies , both experimental and theoretical. In aerospace engineering , it has been necessary to study the aerodynamics in high angles of attack because the aircraft , rocket and space transportation vehicle and so on have been used widely , and there are necessary to have higher angles of attack to use them efficiently. In order to better understand three-dimensional flow separation, several groups have studied the flow about a 6 to 1 prolate spheroid at angle of attack. This flow is a well-defined, relatively simple 3-D flow which exhibits all the fundamental phenomena of three-dimensional flow. The experiments performed in air by Kreplin et al.[2)~5)] were extensively exploited. These experiments constituted several particularly well-documented test cases, including wall pressure and wall shear stress as well as detailed flow probings with multihole pressure probe.These experiments were conducted for two incidences : 10 and 30deg. More recently, Chesnakas et al.[6)] have documented the quantitative properties of separation line on the prolate spheroid measuring the distribution of velocity and Reynolds stress near separation line using laser doppler velocimeter. In the visualization experiments, the variations of the structure for separated vortices in each section over slender bodies have been shown using

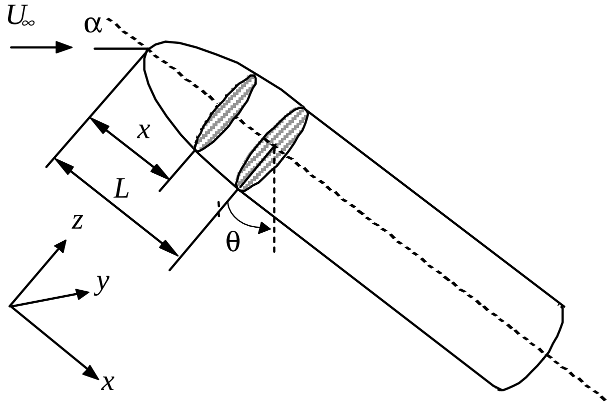

Fig.1 Model and coordinate system

laser light sheet method and tracer method in detail by Kubota et al.[1]. There have been few efforts to considerate quantitatively for the vortices which are recognized by visualization picture. The aim of the present study is the evaluation of the position for the vortex core and the turbulence intensity in the longitudinal vortices quantitatively using visualization technique and hot wire anemometer which has X-type probe.

2 Experimental setup

The wind tunnel used in this study is the Gottingen type. The test section is 400×400 mm, and length of the section is 650mm. The model was made of stainless-steel. This model is an axisymmetric paraboloid , whose radius r is represented by $r = \sqrt{x}$ with x , the axial distance from the vertex of the model. The nose length L of the model is 140mm, and at the position of x=L diameter D is 75mm. The model is coaxially connected to a 300mm length cylinder as shown in Fig.1.

3 Experimental approach

3.1 Visualization experiments using fog machine

In this study, tracer method was used as visualization technique.Fog machine was placed in upstream of 4m from the test section. Since the dence smoke was obtained by this machine, we could observe the separated flow behind the model in detail. Argon-ion laser,of which the maximum power is 6w , was used as light source. The beam diameter of laser light is 1.5 mm , and the light sheet whose thickness is 3 mm was obtained by connecting fiber-link and hemi-cylindrical lens. This light sheet illuminates normal to the body surface. In this experiment, 18 sections are visualized from x/L =0.07 to 1.0. Visualization system is shown in Fig.2.

3.2 Velocity measurements using hot wire anemometer

The hot wire anemometer in this experiment is the type of constant temperature. The average and fluctuation of velocity fields around the body was measured by this apparatus. Fig.3 shows measurement system using hot wire anemometer. This system consists of two constant temperature velocimetry units and a unit measuring temperature for temperature compensation. Measuring points are nine with equal spacing 11.25° at 90°<θ <180°. Further two points near secondary vortex which is confirmed by visualization picture[7)8)] are added for measuring ponit. In z-direction measuring points are 30 from neighbourhood of the body surface to external flow region. X-type probe was used , which velocity vectors and velocity fluctuation are calculated. The procedure used for measuring was as follows. We use two probes and measure changing the probe arrangement : first the tungsten-wire in the vertex of the probe is placed in x-y plane(UV probe) , next after that by rotating UV probe for

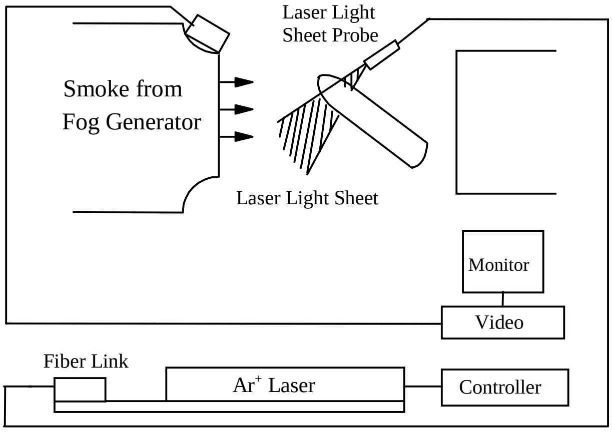

Fig.2 Visualization system

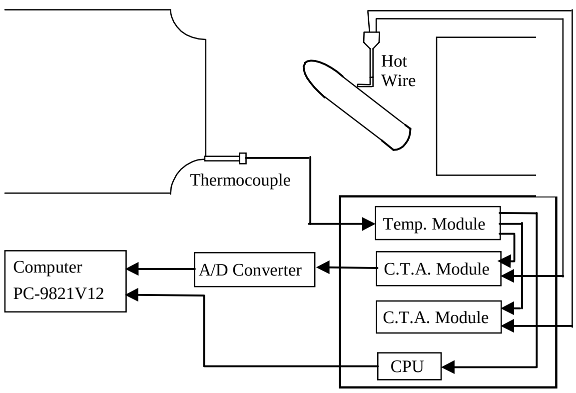

Fig.3 Measurement system using hot wire anemometer

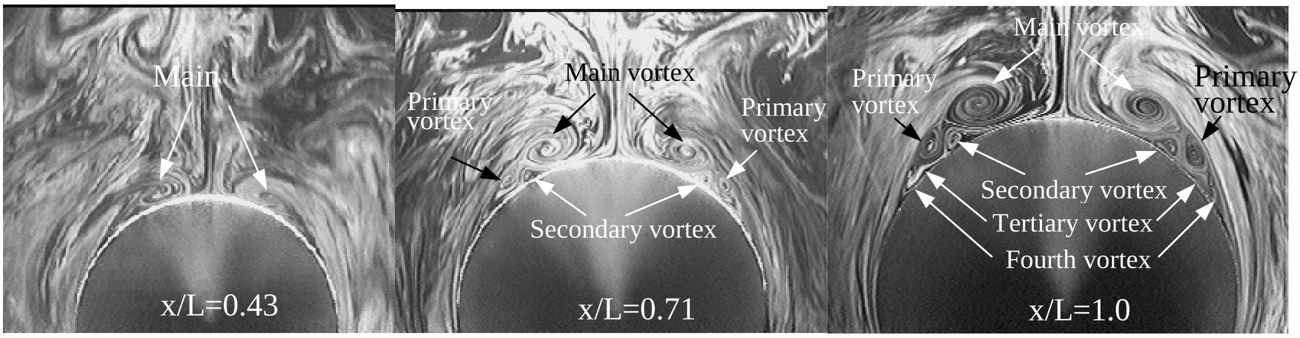

Fig.4 Visualization pictures(α=30°, Re=9.0×10^3)

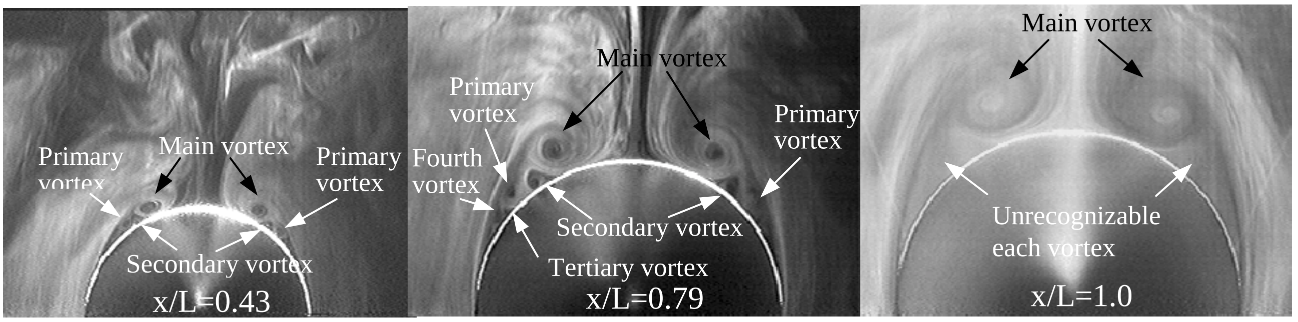

Fig.5 Visualization pictures(α=40°, Re=1.8×10^4)

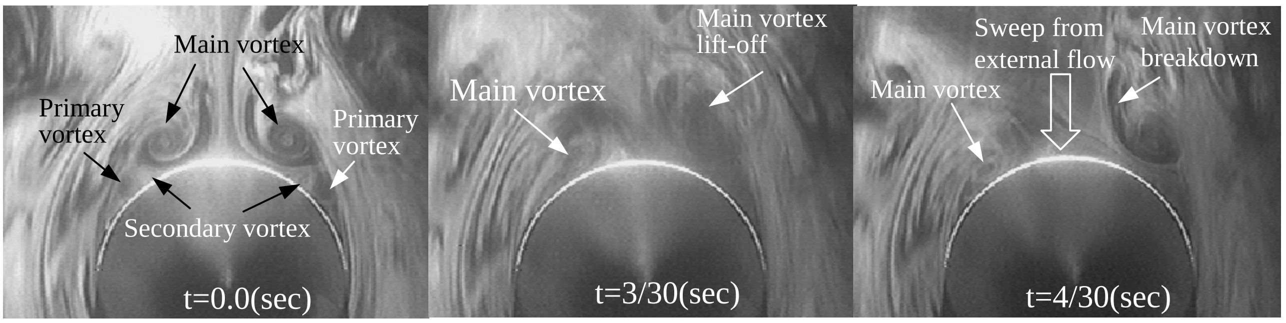

Fig.6 Visualization pictures(α=50°, Re=9.0×10^3, x/L=0.57)

90 degree tungsten-wire is placed in *x-z* plane(UW probe). Three dimensional velocity components are evaluated in these procedure. In this experiment sampling frequency is 4kHz , and data number is 16,384.

4 Results and Discussion

4.1 Visualization using fog machine

In this experiment, angles of incidence was set for 30,40 and 50 deg. Main flow velocities are 1.8m/s and 3.6m/s : Reynolds numbers are 9.0×10^3 and 1.8×10^4 respectively reffered to 75mm base-diameter at x=L=140mm.Fig.4 shows visualization pictures at 30° of angle of attack and Re=9.0×10^3. Main vortex is found at x/L=0.43 and primary , secondary and tertiary vortices are generated mutual interventionally with increasing x/L. Five vortices from main vortex to fourth vortex exist symmetrically at x/L=1.0. The flows which supply the vorticity these vortices are the primary separation flow near θ=90° and the reattachment flow near θ=180°. The influence of the reattachment flow increases with an increase in x/L. Fig.5 shows visualization pictures at 40° of angle of attack and Re=1.8×10^4. Primary and secondary vortices are already observed at x/L =0.43 which has not been shown at 30° of angle of attack. At x/L=0.79, it has been identified from primary vortex to fourth vortex. The vortices except main vortex are unrecognizable at x/L=1.0. This fact indicates the turbulent intensity increases in this region. Fig.6 shows

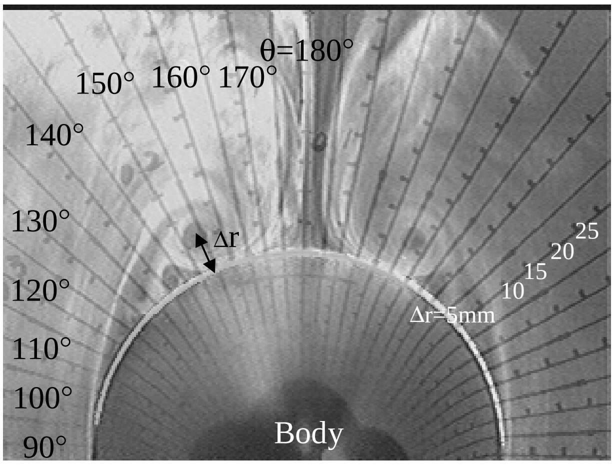

Fig.7 Synthesized image of visualization picture and polar coordinate around the body

visualization pictures at 50° of angle of attack and Re=9.0×10^3. It is shown that the vortices transform unsteadily : the size of crosswise vortex varies with time. The extensive sweep flow near θ=180° from main stream region to body surface make main vortex break down at t=4/30sec. At the same time, It is found that the flow is more turbulent than α=30° and 40° because primary and secondary vortices are unrecognizable. From these visualization pictures, it is confirmed that the behavior of longitudinal vortices differ in terms of angle of attack and Reynolds number. Here we notice the variation for the position of vortex core. The vortex core is recognized from the flow pattern in the visualization picture. In this experiment, we take a photograph of template picture with polar coordinate. Synthesizing template picture and visualization picture, the vortex core lift-off Δr(mm) could be measured. Fig.7 shows a synthesized picture. Fig.8(a)(b)(c)(d) shows dimensionless value which is obtained to divide Δr by R=37.5mm base-radius at x=L=140mm. From these figures,main vortex lift off the body surface linearly with increasing *x/L*. The ・r/R increases with an increase in angle of attack. While Δr/R decreases with increasing Reynolds number. Though the rate of Δr/ R for primary and secondary vortices with *x/L* are smaller than main vortex, the tendency remains incremental. The variation which means that vortex core lifts off and approaches near body

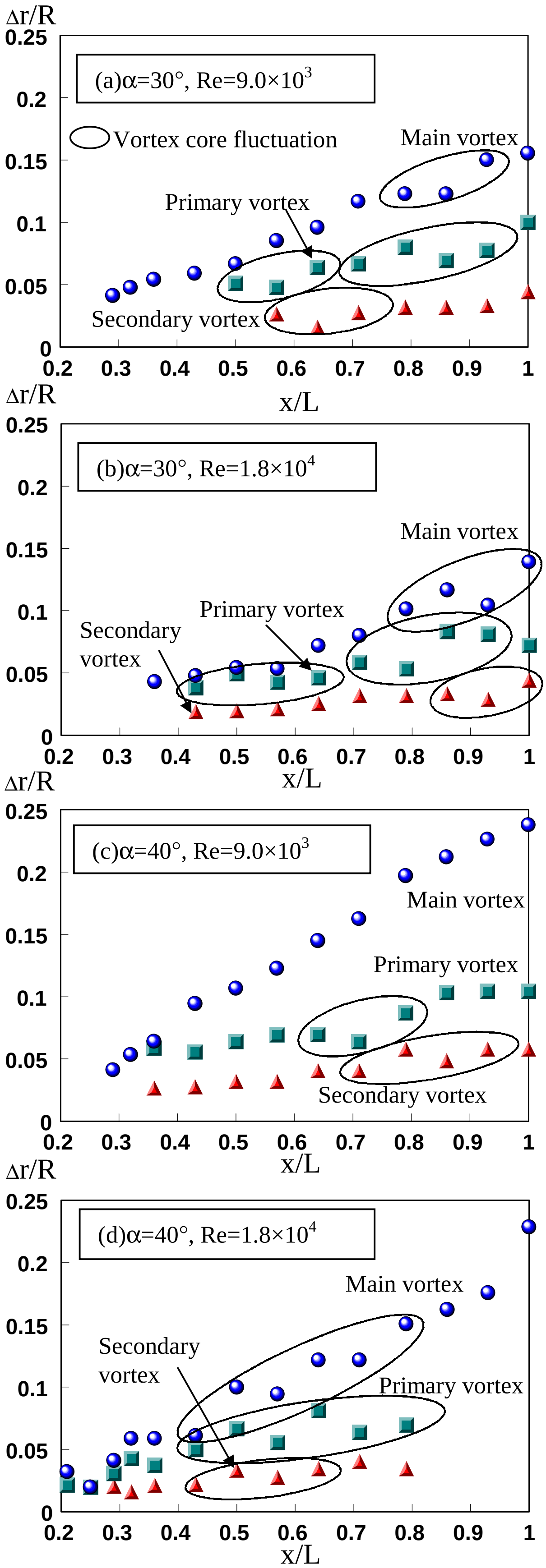

Fig.8 The lift-off of the longitudinal vortices

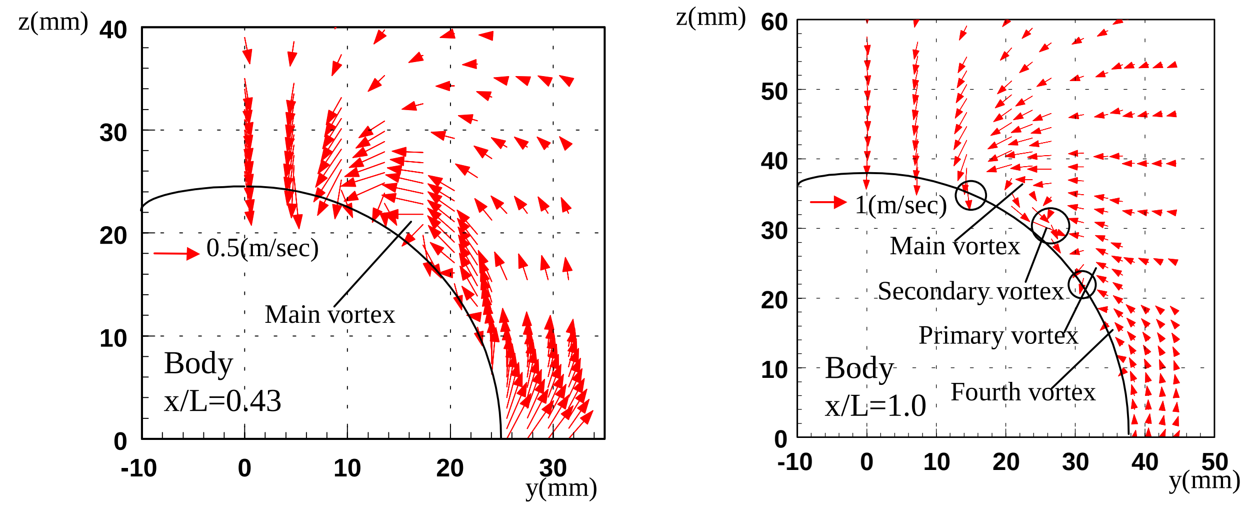

Fig.9 Velocity vectors in y-z plane (α=30°, *Re*=9.0×10^3)

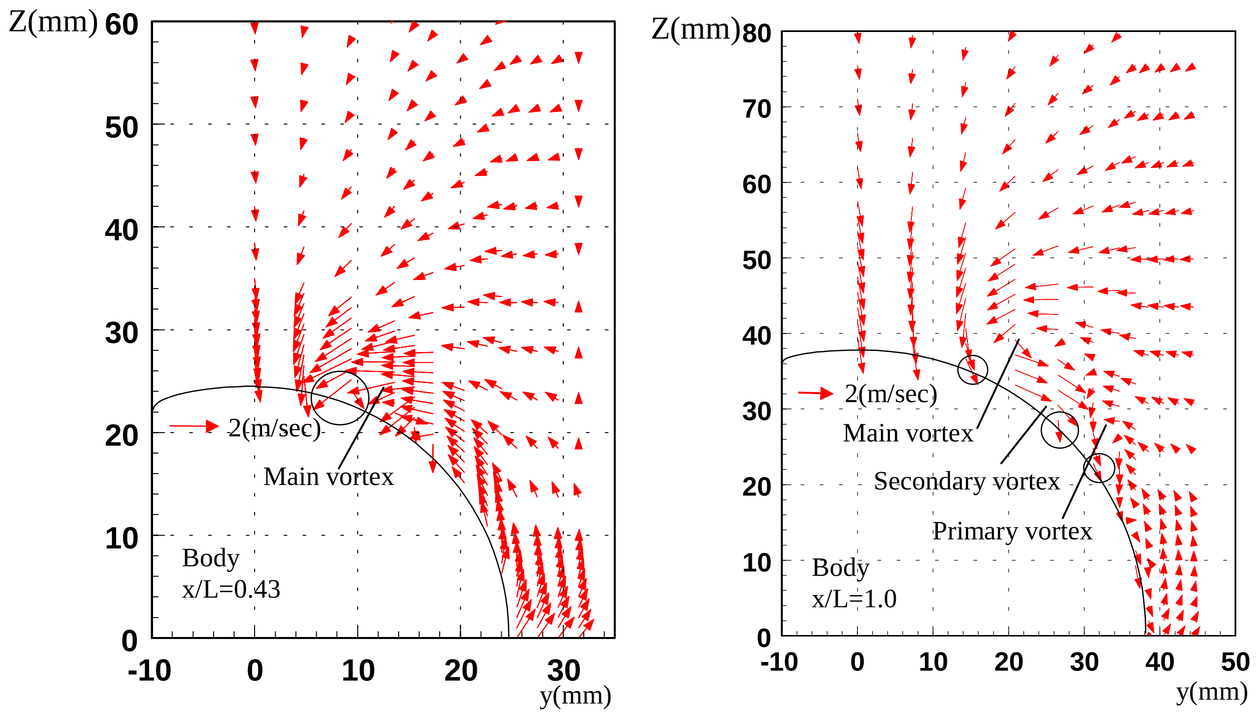

Fig.10 Velocity vectors in *y-z* plane (α=40°, *Re*=1.8×10^4)

surface was observed at *x*/*L*>0.5 which was indicated with circles in Fig.8. The effect of attack angle for primary and secondary vortices is the same tendency as main vortex. The decrease of Δr/R with increasing Reynolds number is not shown for these vortices.

4.2 Velocity measurements using hot wire anemometer

In this study average and fluctuation of velocity fields have been assessed using hot wire anemometer which has two X-type probes under the same conditions as the visualization experiments mentioned above. The quantitative properties of the longitudinal vortices have been investigated. The residual turbulence of wind tunnel in this experiment is 0.7% in the case of U_∞=1.8m/sec , and 1.1% in the case of U_∞=3.6m/sec. The uniformity of velocity profile at the test section of the wind tunnel is 0.8% in the case of U_∞=1.8m/sec , and 2.6% in the case of U_∞=3.6m/sec. Fig.9 shows velocity vectors at 30° of angle of attack and Re=9.0×10^3. The primary and fourth vortices are shown at *x*/*L*=1.0 which has not been shown at *x*/*L*= 0.43. The secondary vortex is validated

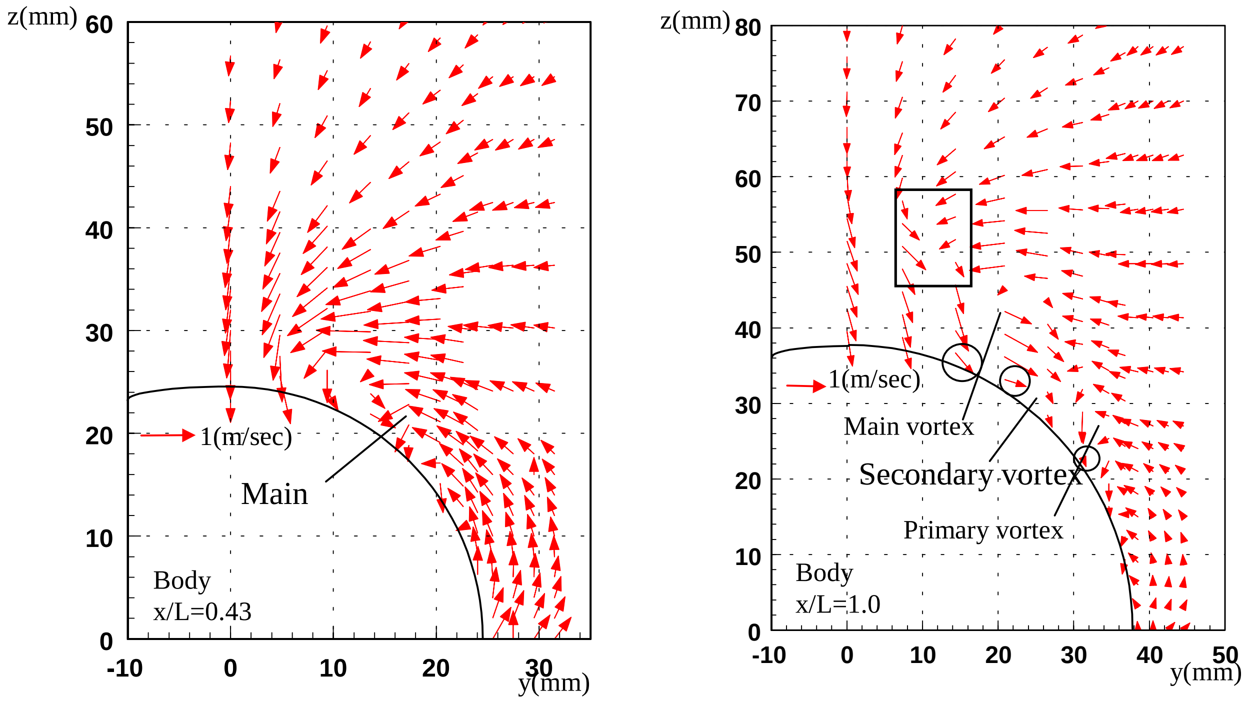

Fig.11 Velocity vectors in *y-z* plane (α=50°, *Re*=9.0×10^3)

in the upper half of it because the core of secondary vortex exists near body surface. These velocity vectors are in good agreement with visualization pictures in Fig.4. Fig.10 shows velocity vectors at 40° of angle of attack and Re=1.8×10^4. The primary and secondary vortices which has been observed in visualization picture, are not found in this velocity vectors. This discrepancy is attributed that the size of vortices is smaller than the distance of two hot wires. At *x*/*L*=1.0 the primary and secondary vortices in the velocity vectors are confirmed. The region of main vortex at *x*/*L*= 1.0 is larger than that at *x*/*L*= 0.43. Noting the reattachment flow near θ=180°, it should be mentioned that the velocities of z-direction are large relatively to those near θ=157.5°. This fact can be related to the extension of main vortex. From the velocity vectors at *x*/*L*= 1.0, it is shown that the velocity in y-direction is large after secondary separation occurs near θ=146.25°, and the region of circumferential reversal flow becomes extendable to θ=90° after secondary vortex reattaches near θ=123.75°. Fig.11 shows velocity vectors at 50° of angle of attack and Re=9.0×10^3. Though the primary and secondary vortices are unrecognizable at *x*/*L*= 1.0 , these vortices in the average velocity vectors are recognizable. The difference between α=40° and α=50° is the flow discontinuity in the region which shows a square in Fig.11. In this region , It suggests that the large fluctuation of velocity exists since y-directional velocity component of adjacent velocity vectors is inverse , and the primary separation flow and the reattachment flow from external flow become confluent. Because in the turbulent reattachment flow the separation does not occurs easily , the size of the region for secondary vortex becomes decremental. The velocity vector corresponding to each longitudinal vortex is recognizable in the velocity distribution shown from Fig.9 to Fig.11. We notice the fluctuation wave forms in each longitudinal vortex near body surface at any *x*/*L*, Reynolds numbers and angles of attack. The noting vectors are shown with circles in Fig.9 to Fig.11. Fig.12 shows the chart of fluctuation wave forms. Here fluctuation wave form shows the variation of *v*: y-directional velocity component. The tendency of *u* and *w* is the same as *v*. From this chart , the

α	*Re*	*x*/*L*	Main vortex	Primary vortex	Secondary vortex
40°	1.8×10^4	0.43	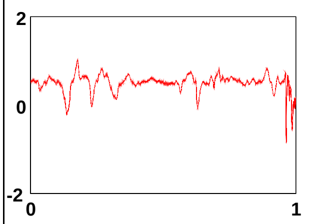	N.A.	N.A.
		0.86	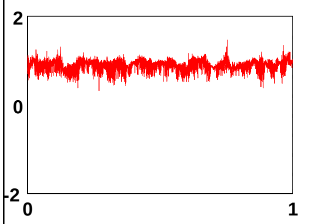	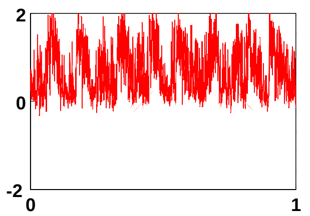	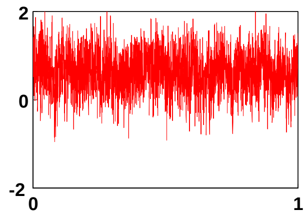
		1.0	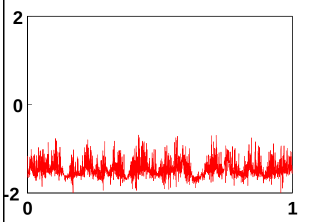	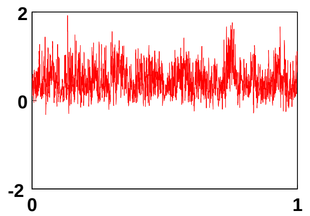	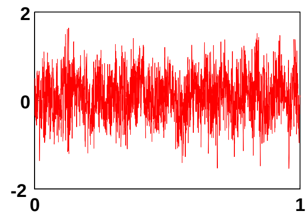
30°	9.0×10^3	1.0	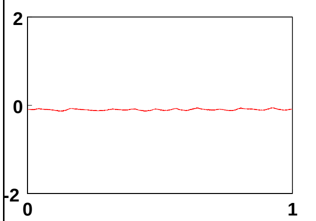	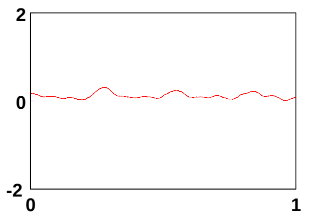	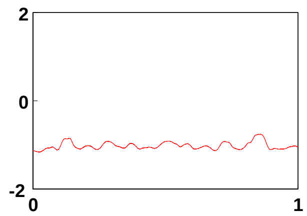
50°	9.0×10^3	1.0	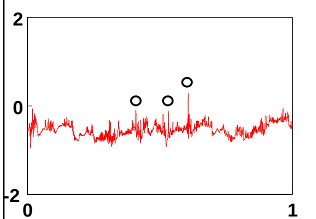	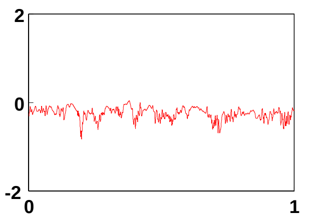	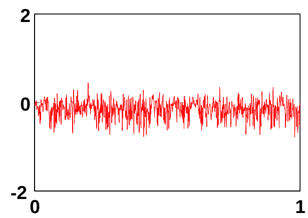

Fig.12 Wave forms of velocity fluctuation in longitudinal vortices

velocity fluctuation in the secondary vortex is maximum in every attack of angle. The velocity fluctuation in the main vortex is minimum. At α=40°, It is confirmed that the cycle of fluctuation becomes shorter with increasing *x*/*L*. The secondary vortex at *x*/*L*=1.0 in α=40° and α=50° grows fully turbulent. While in α= 30° the fluctuation of low frequency is still observed at *x*/*L*=1.0. The large fluctuation exists intermittently at α=50°(circles in Fig.12), this finding shows that strong sweep from external flow shown in Fig.6 is demonstrated quantitatively. Fig.13 shows r.m.s. distribution at *x*/*L*=0.43,1.0. The r.m.s. value in this figure is sum of three directional r.m.s. values , and is transformed dimensionless with uniform velocity U_∞. The r.m.s. value is maximum at θ=123.5° where primary separation occurs , in the case of *x*/*L*=0.43 and α=30°. On the contrary, in α=40° and 50° the r.m.s. value grows large in each θ, at which the primary and secondary vortices exists : the distribution profile with θ has two vertexes. At *x*/*L*=1.0 the r.m.s. value is maximum in the region of secondary vortex , and the distribution profile which is observed at *x*/*L*=0.43 disappears. The r.m.s. value increases with increase in angles of attack. Further the r.m.s. value increases as *x*/*L* increases.

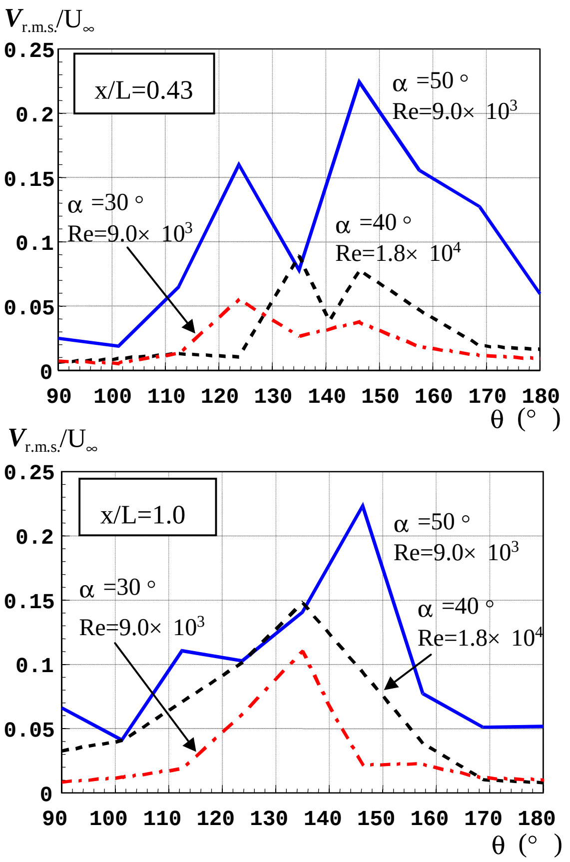

Fig.13 r.m.s. distribution

5 Conclusions

In this study, we have investigated the separated vortices over axisymmetric paraboloid at high angles of attack. Visualization pictures has been obtained using fog machine and laser light sheet.Mean and fluctuation velocity distribution have been measured using hot wire anemometer which has X-type probe. The following conclusions were derived from the results and discussion.

(1)The process of formation for longitudinal vortices from main vortex to forth vortex was confirmed. It was shown that the rate of growth for vortices increases with increasing angle of attack. The phenomenon of breakdown in main vortex occurs unsteadily in α=50°.

(2)The positions of core in longitudinal vortices has been estimated quantitatively by synthesizing visualization picture using fog machine and template picture which shows polar coordinate around the body. It has been found that the core of main vortex lifts off the body surface linearly with increasing *x*/*L*. While It has been identified that the core of primary and secondary vortex approach and lift off the body surface with increasing *x*/*L*.

(3)Three dimensional average velocity vectors has been calculated using two X-type probes in hot wire anemometer which is the type of constant temperature. As a result , we can assess the longitudinal vortices quantitatively. The variation of the size for longitudinal vortices and the region of back flow has been evaluated.

(4)The wave forms of fluctuation velocity with time differ in terms of angle of attack, Reynolds number and type of longitudinal vortices. It has been demonstrated that the r.m.s. value has a maximum in the region of secondary vortex in each angle of attack.

6 References

[1] Jia,M.,Watanuki,T. and Kubota,H.:The Visualization of Separated Flow over Slender Bodies at High Angles of Attack, J.Visualization Soc. Jpn.,14(1994), pp.243-252

[2] Kreplin, H.P. and Vollmers, H.: Preliminary Turbulence Measurements in Three-Dimensional Boundary Layers on a Prolate Spheroid , DFVLR- AVA-Report IB 222 81 CP1(1981), pp.218-229

[3] Meier, H.U. and Kreplin, H.P. : Experimental Investigation of the Boundary Layer Transition and Separation on a Body of Revolution , Z.Flugwiss.Weltraumforsch. 4 (1980), pp.65-71

[4] Kreplin, H.P. and Hohler, G. : Application of the Surface Hot Film Technique to Laminar Flow Investigations,DGLR-Bericht 92-06(1992), pp.123-131

[5] Kreplin, H.P. and Stager, R. : Measurements of the Reynolds-Stress Tensor in the Three-Dimensional Boundary Layer of an Inclined Body of Revolution ,Proc. of Ninth Symposium on "TURBULENT SHEAR FLOWS" , Kyoto, Japan(1993), pp.2.4.1-2.4.6.

[6] Chesnakas, C.J. and Simpson, R.L.: Measurements of the Turbulence Structure in the Vicinity of a 3-D Separation, Trans. ASME,118(1996), pp.268-275

[7] Ishide, T. and Nishikawa, N. : Experimental Study of Unsteady flow behavior in Separated Flow along Blunt Body , Proc. of 31st Aircraft Symposium.,1993, pp.140-143

[8] Ishide, T. and Nishikawa, N. : The Visualization and Numerical Analysis of Separated Flow over Axisymmetric, Paraboloid , Proc. of 34th Aircraft Symposium,1996, pp.11-14

[9] Nishikawa, N. and Ishide, T. : Visualization and Measurement of Separated Flow , Proc.of The Second Asian-Pacific Conference on Aerospace Technology and Science, Dun Huang(1997), pp.137-142